



Demographic back-casting reveals that subtle dimensions of climate change have strong effects on population viability

Kevin Czachura | Tom E. X. Miller

Program in Ecology and Evolutionary
Biology, Department of BioSciences, Rice
University, Houston, TX, USA

Correspondence

Tom E. X. Miller
Email: tom.miller@rice.edu

Funding information

Division of Environmental Biology, Grant/
Award Number: 1440478, 1655499,
1748133, 1754468 and 1543651

Handling Editor: Roberto Salguero-Gómez

Abstract

1. The effects of climate change on population viability reflect the net influence of potentially diverse responses of individual-level demographic processes (growth, survival, regeneration) to multiple components of climate. Articulating climate–demography connections can facilitate forecasts of responses to future climate change as well as back-casts that may reveal how populations responded to historical climate change.
2. We studied climate–demography relationships in the cactus *Cylindriopuntia imbricata*; previous work indicated that our focal population has high abundance but a negative population growth rate, where deaths exceed births, suggesting that it persists under extinction debt. We parameterized a climate-dependent integral projection model with data from a 14-year field study, then back-casted expected population growth rates since 1900 to test the hypothesis that recent climate change has driven this population into extinction debt.
3. We found clear patterns of climate change in our central New Mexico study region but, contrary to our hypothesis, *C. imbricata* has most likely benefitted from recent climate change and is on track to reach replacement-level population growth within 37 years, or sooner if climate change accelerates. Furthermore, the strongest feature of climate change (a trend towards years that are overall warmer and drier, captured by the first principal component of inter-annual variation) was not the main driver of population responses. Instead, temporal trends in population growth were dominated by more subtle, seasonal climatic factors with relatively weak signals of recent change (wetter and milder cool seasons, captured by the second and third principal components).
4. *Synthesis.* Our results highlight the challenges of back-casting or forecasting population dynamics under climate change, since the most apparent features of climate change may not be the most important drivers of ecological responses. Environmentally explicit demographic models can help meet this challenge, but they must consider the magnitudes of different aspects of climate change alongside the magnitudes of demographic responses to those changes.

KEYWORDS

Cactaceae, climate change, demography, extinction debt, integral projection model, long-term ecological research

1 | INTRODUCTION

Population extinction debt is likely to increase in frequency as a fingerprint of global change, including climate change (Dullinger et al., 2012; Urban, 2015). Extinction debt is a form of transient dynamics whereby populations persist despite having population growth rates that fall below replacement level ($\lambda < 1$), suggesting a long-term trajectory towards local extinction but with potentially long time-lags (Hastings et al., 2018; Kuussaari et al., 2009). While extinction debt is often studied through species richness patterns at the community level (e.g. Vellend et al., 2006), there is recent emphasis on the underlying single-species dynamics whereby populations transition from positive to negative growth rates (Hylander & Ehrlén, 2013; Lehtilä et al., 2016). In the absence of significant migration (which can maintain populations in sink habitats), extinction debt suggests that the environment was more favourable for population growth at some time in the past. However, the mechanisms that cause populations to tip from positive to negative growth rates are rarely known, and this information may be critical for effective conservation planning (Hylander & Ehrlén, 2013).

Structured population models built from individual-level demographic rates provide a powerful framework for studying the drivers of extinction debt (Lehtilä et al., 2016) and environment-dependent population dynamics more generally (Ehrlén & Morris, 2015). By incorporating climatic factors as statistical covariates, previous studies have identified climatic limits of population viability and forecasted responses to particular types of climate change (e.g. Adler, Byrne, & Leiker, 2013; Jenouvrier et al., 2014; Maschinski, Baggs, Quintana-ascencio, & Menges, 2006). Additionally, articulating the connections between environment and demography can allow for 'back-casting' population dynamics into historical environmental regimes; while rarely done (Smith, Caswell, & Mettler-Cherry, 2005), this approach may provide valuable insight regarding when and why populations fell into extinction debt.

Many studies of climate–demography relationships focus on single climate variables that are known to be a dominant component of climate change and/or known to have a strong influence on the focal species (e.g. Iler et al., 2019; Jenouvrier et al., 2009; Van de Pol et al., 2010). However, for many species, it is not always apparent a priori which dimensions of climate are most important, and this poses challenges for predicting population responses to climate change. Previous studies have shown that different components of climate change may have independent effects on different aspects of demography or physiology (Buckley & Kingsolver, 2012; Frederiksen, Daunt, Harris, & Wanless, 2008; Lynch et al., 2014; Van de Pol et al., 2010). Furthermore, different life stages (e.g. young versus old) and different vital rate processes (e.g. growth, survival, reproduction) may differ in the magnitude and even direction of their responses to single climate drivers (Doak & Morris, 2010; Dybala, Eadie, Gardali, Seavy, & Herzog, 2013; Morrison & Hik, 2007; Tenhumberg, Crone, Ramula, & Tyre, 2018), and single life stages

or vital rates may be affected by multiple drivers (Dagleish, Koons, Hooten, Moffet, & Adler, 2011; Frederiksen et al., 2008; Sletvold, Dahlgren, Øien, Moen, & Ehrlén, 2013; Williams, Jacquemyn, Ochocki, Brys, & Miller, 2015). Ultimately, the influence of climate on population growth depends on the sensitivities of vital rates to climate drivers and the sensitivities of λ to the vital rates, integrated across the life cycle (Ådahl, Lundberg, & Jonzen, 2006; McLean, Lawson, Leech, & van de Pol, 2016). These complications, common to environmentally explicit demographic studies (Ehrlén, Morris, von Euler, & Dahlgren, 2016), highlight the value of leveraging long-term data to gain resolution of climate drivers and the importance of accounting for demographic complexity across the life cycle.

We used long-term demographic data to study climate-dependent population dynamics of a long-lived Chihuahuan desert cactus persisting under extinction debt. Our previous work with the tree cholla cactus (*Cylindropuntia imbricata* Haw. D.C.) (Cactaceae) indicated, with >95% certainty, that our focal population in the northern Chihuahuan Desert (New Mexico, USA) is in decline (stochastic population growth rate $\lambda_s < 1$) despite current densities that are reasonably high (Elder & Miller, 2016; Miller, Louda, Rose, & Eckberg, 2009; Ohm & Miller, 2014). This region has experienced strong climatic fluctuations over the past century, including several decadal-scale droughts interrupted by relatively wet periods (Peters, Havstad, Archer, & Sala, 2015).

Our study was conducted in the following steps. First, we characterized climate variation and change in our northern Chihuahuan desert study region over the past century. Second, we estimated vital rate responses to inter-annual climate variation during the demographic study period (2004–2017). We hypothesized that high-sensitivity vital rates (those that strongly influence λ) would be less responsive to environmental variability than low-sensitivity vital rates (Pfister, 1998). Third, we back-casted climate-dependent demography to determine whether the past century included periods that were favourable for population growth, thus testing the hypothesis that recent climate change has driven this population into extinction debt. Our analysis relied on a Bayesian framework that incorporates key sources of uncertainty into our back-cast. Finally, we asked whether the components of climate that are changing most strongly in this system are the same climate components that most strongly influence cactus demography.

2 | MATERIALS AND METHODS

2.1 | Focal species, study site and demographic data collection

Tree cholla cactus is widely distributed throughout desert and grassland habitats of the southwest United States and northern Mexico. These long-lived plants (40-plus years) grow through the production and elongation of cylindrical stem segments. These vegetative structures as well as flowerbuds are initiated in late spring. Flowering occurs in early summer and stem segment elongation takes place during the remainder of the growing season. For

climate analyses, we divide the calendar year into warm-season months (May through September), when stem elongation, flowering and seed production occur, and cool-season months (October through April).

This study was conducted at the Sevilleta National Wildlife Refuge (SNWR), a Long-Term Ecological Research site (SEV-LTER) in central New Mexico and near the centre of this species' geographic distribution. Our study population occurs in the Los Piños mountains at an elevation of 1,790 m. Tree cholla are a dominant component of the vegetation in this area (0.1 m^{-2} ; Miller et al., 2009), along with oaks, yucca, Piñon pine and the grasses *Bouteloua gracilis* and *B. eriopoda*.

The present study relies on long-term (2004–2017) demographic data on individual-level measures of growth, survival and reproduction recorded from tagged plants in the Los Piños population that were censused in late May each year. This was a pre-breeding census that corresponds to the initiation of vegetative and reproductive structures (Figure C1). We treat May 1 as the start of the transition year (coincident with the start of the warm-season months). There were a total of 1,172 unique individuals in the dataset and 7,442 transition-year observations from four to eight plots or spatial blocks depending on the year. Full details of the study design and data collection are given elsewhere (Elder & Miller, 2016; Miller et al., 2009; Ohm & Miller, 2014).

2.2 | Climate data

Our goal was to connect inter-annual variation in demography to corresponding variation in temperature and precipitation. SEV-LTER collects climate data from a network of meteorological stations throughout SNWR. While the SEV-LTER climate data cover years of our demographic data collection, our intention was to back-cast demographic performance farther back into the 20th century. We therefore gathered climate data from ClimateWNA v5.60 (Wang, Hamann, Spittlehouse, & Carroll, 2016), a software package that uses PRISM (Daly et al., 2008) and WorldClim (Hijmans, Cameron, Parra, Jones, & Jarvis, 2005) data to calculate downscaled data for western North America based on location and elevation, going as far back as 1900. We derived seasonal estimates (warm- and cool-season) of total precipitation and mean, minimum and maximum temperature from monthly climate data, for a total of eight variables. Months were aligned to correspond to demographic transition years rather than calendar years, which means the cool-season climate for a transition year beginning in May of year t spans October of year t through April of year $t + 1$ (Figure C1).

To reduce the dimensionality of the climate data, we conducted principal component analysis (PCA) on the eight climate variables for the years 1900–2017, with climate values scaled to unit variance. We estimated the variance in the raw climate data explained by each PC and the variable loadings, which give the correlations between original variables and PC values. PCA allowed us to rank the magnitudes

of multiple aspects of climate variation and change by examining how warm- and cool-season variables loaded onto the ranked PC axes.

By relying on downscaled, interpolated climate data instead of direct observations from meteorological stations we are trading off local resolution in favour of more historical years of data. We quantified this loss of resolution by comparing predictions from ClimateWNA to SEV-LTER data for years that they overlapped, using the SEV-LTER meteorological station that was nearest our study population (Appendix A). We found that the two datasets were generally well-correlated (Table A1; Figures A1 and A2), which bolstered our confidence in ClimateWNA for back-casting demographic responses to climate over the historical record. We further explored the implications of using downscaled data by repeating all of our analyses (described next) with SEV-LTER meteorological data and comparing results between the two data sources (Appendix A).

2.3 | Statistical estimation of climate dependence

We fit generalized linear mixed effects models in a hierarchical Bayesian framework to quantify climate dependence in demographic vital rates, as captured by three principal components of climatic variability. The choice of three PCs was based on the results of parallel analysis (Figure A3), a statistical method for determining how many components to retain (Franklin, Gibson, Robertson, Pohlmann, & Fralish, 1995). There were four vital rates measured in the long-term study for which we could estimate climate dependence: survival from year t to year $t + 1$, individual growth (change in size from year t to year $t + 1$), probability of flowering in year t and the number of flowerbuds produced year in t , given that a plant flowered. Survival and growth from year $t - 1$ to t were dependent on size in year $t - 1$, and the climate covariate corresponded to the climate year $t - 1$ to t . Reproductive status and fertility in year t were dependent on size in year t and on climate from $t - 1$ to t . This timing of size and climate effects was intended to match processes in the population model (Figure C1). We did not quantify climate dependence in seedling recruitment. While we searched plots each year and added newly detected plants to the census, we could not confidently assign a birth year to these new additions (seedlings require several years of growth before they are consistently detectable in our census) so we do not know the climatic conditions under which they recruited.

All of the models for climate-dependent vital rates used the same linear predictor for the expected value (μ) but applied a different link function ($f(\mu)$) depending on the distribution of the observations:

$$f(\mu) = \beta_0 + \beta_1 x + \rho_1^1 \text{PC1} + \rho_2^1 \text{PC1}^2 + \rho_3^1 x \text{PC1} + \rho_1^2 \text{PC2} + \rho_2^2 \text{PC2}^2 + \rho_3^2 x \text{PC2} + \rho_1^3 \text{PC3} + \rho_2^3 \text{PC3}^2 + \rho_3^3 x \text{PC3} + \phi + \tau. \quad (1)$$

The linear predictor includes an intercept (β_0) and size slope (β_1). The size variable x is the natural logarithm of plant volume ($\log_e(\text{cm}^3)$),

which was standardized to mean zero and unit variance for analysis. Other fixed-effect coefficients (ρ) correspond to climate variables and climate \times size interactions. We include quadratic terms for climate to account for the possibility of non-monotonic climate responses. Climate coefficient (ρ) superscripts correspond to each PC, and subscripts correspond to linear, quadratic and size-interaction effects. Finally, the linear predictor includes normally distributed random effects for plot-to-plot variation ($\phi \sim N(0, \sigma_{\text{plot}})$) and year-to-year variation ($\tau \sim N(0, \sigma_{\text{year}})$). The year random effect can be interpreted as inter-annual variability in demography that cannot be explained by the climate PCs. We used stochastic variable selection in a Bayesian framework to reduce model complexity, dropping coefficients that were effectively zero with $\geq 90\%$ certainty. Complete methods for variable selection are provided in Appendix B.

The growth data were assumed to be normally distributed; this model applied the identity link and included an additional parameter for residual variance. We explored size dependence in the residual variance of growth (which determines how individuals are distributed around their expected future size) but found that this led to poorer model fits, so we proceeded to assume a constant value. The survival and flowering data were Bernoulli distributed, and these models applied the logit link function. The fertility data (flowerbud counts) were modelled as Poisson distributed, including an individual-level random effect to account for overdispersion. All coefficients were given vague priors. We evaluated model fits using posterior predictive checks (Elder & Miller, 2016). All models were fit using JAGS (Plummer, 2003) and R2JAGS (Su & Yajima, 2012). Analysis code is available at https://github.com/texmiller/cholla_climate_IPM.

2.4 | Demographic modelling

2.4.1 | Model description

The statistical models described above formed the backbone of the integral projection model (IPM) that we used to estimate population growth in variable climate environments. Following previous studies (Compagnoni et al., 2016; Elder & Miller, 2016; Ohm & Miller, 2014), we modelled the life cycle of *C. imbricata* using continuously size-structured plants, $n(x)$, and two discrete seed banks ($B_{1,t}$ and $B_{2,t}$) corresponding to 1- and 2-year-old seeds:

$$B_{1,t+1} = \kappa \delta \int_L^U P(x, \mathbf{c}_{t-1}; \alpha_t^P) F(x, \mathbf{c}_{t-1}; \alpha_t^F) n(x)_t dx, \quad (2)$$

$$B_{2,t+1} = (1 - \gamma_1 B_{1,t}). \quad (3)$$

Functions P and F give the probability of flowering and the number of flowerbuds produced, respectively, for an x -sized plant. The vector \mathbf{c}_{t-1} contains the climate PC values for climate year $t - 1$, which affects flowering and fertility in year t , and hence the 1-year-old seed bank in year $t + 1$. Parameters α_t^P and α_t^F are random year effects estimated

from the statistical models. The integral is multiplied by the number of seeds per fruit (κ) and probability of seed dispersal/survival (δ) to give the number of seeds that enter the 1-year-old seed bank. Parameters L and U are the lower and upper bounds, respectively, of the plant size distribution. Plants can recruit out of the 1-year-old seed bank with probability γ_1 or transition to the 2-year old seed bank with probability $(1 - \gamma_1)$. Seeds in the 2-year-old seed bank are assumed to either germinate (probability γ_2) or die. Continuous-size dynamics were given by:

$$n(y)_{t+1} = (\gamma_1 B_{1,t} + \gamma_2 B_{2,t}) \eta(y) \omega + \int_L^U S(x, \mathbf{c}_t; \alpha_t^S) G(y, x, \mathbf{c}_t; \alpha_t^G) n(x)_t dx. \quad (4)$$

The first term indicates recruitment from the seed banks to size y , where $\eta(y)$ gives the seedling size distribution, assumed normal with mean μ_s and standard deviation σ_s . Mortality between germination (late summer) and the yearly demographic census (May) is accounted for with survival probability ω . In the second term, functions S and G give the probabilities of surviving to year $t + 1$ and growing to size y , respectively, for an x -sized plant in year t . Climate dependence and random year effects are included as in Equation 2, except the timing of climate effects is shifted such that growth and survival from t to $t + 1$ are affected by climate over the same interval (Figure C1). As above, survival and growth functions also take time-varying random intercepts. Field data used to estimate seed and seed bank parameters are described elsewhere (Compagnoni et al., 2016; Elder & Miller, 2016). All parameter estimates are provided in Table C1.

2.4.2 | Model analysis

For analysis, we discretized x into b bins, replacing the continuous kernel with a b -by- b matrix (because our model also included two additional discrete states, the final projection matrix had dimensions $b + 2$ -by- $b + 2$). We used $b = 200$ bins. We extended integration limits L and U to avoid unintentional 'eviction' (Williams, Miller, & Ellner, 2012).

We estimated the asymptotic population growth rate λ as the dominant eigenvalue of the discretized IPM kernel. We compared the observed size distribution and the predicted distribution at the long-term mean climate ($PC_1 = PC_2 = PC_3 = 0$) and found generally good agreement (Figure C2). We then evaluated how λ responded to climate variation by first varying each climate PC independently, holding the other two fixed at their long-term mean. Second, we back-casted λ over the entire climatological record that we had available (1900–2017), which generated a time series of λ_t . We used linear regression to test for temporal trends in λ over this period. We incorporated two types of uncertainty into back-casted values of λ : imperfect knowledge of the parameter values ('estimation error') and year-to-year fluctuations that were not related to climate ('process error'); the latter was estimated from the variances of random year effects. For the years of demographic data collection (2004–2017), we additionally

quantified the deviations between predicted λ based solely on climate and ‘observed’ λ that reflects climate and non-climate year effects (quotations indicate that these are the asymptotic predictions given the vital rates observed in that year). We also conducted a similar analysis of λ_s using a 10-year sliding window (Appendix C) and we explored the consequences of extrapolating vital rate responses to climate values more extreme than those observed during the study period (Appendix D).

Finally, we used life table response experiments (LTREs) to decompose which combinations of climate PCs and vital rate responses were most strongly responsible for temporal fluctuations in the back-casted time series λ_t . We used a fixed-design LTRE (Caswell, 2001) where λ_t was defined as a linear function of climate predictors:

$$\lambda_t = \bar{\lambda} + \sum_{i=1}^3 v_i PC_{i,t}. \tag{5}$$

There is no error term because, in this analysis, climate PCs are assumed to be the sole drivers of fluctuations in λ_t . The coefficient for each climate PC was approximated as:

$$v_i \approx \sum_{j=1}^n \frac{\partial \bar{\lambda}}{\partial \theta_j} \frac{\partial \theta_j}{\partial PC_i}. \tag{6}$$

The LTRE approximation is based on the product of the sensitivity of λ to the vital rates (θ), evaluated at the long-term mean climate

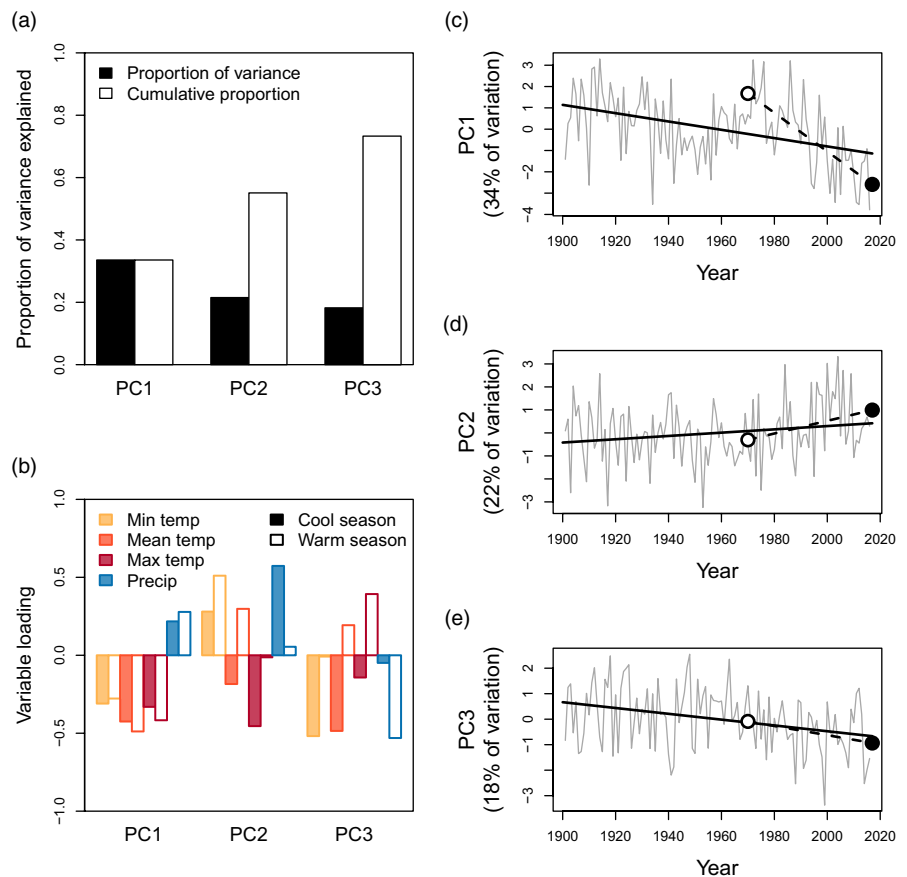
($PC_1 = PC_2 = PC_3 = 0$), and the sensitivity of the vital rates to climate, summed over all vital rates. Because LTRE components are additive, we summed LTRE estimates over the intercept and slope of each vital rate function so that we could interpret the results in terms of vital rate contributions.

3 | RESULTS

3.1 | Climate trends

Three principal components cumulatively explained 73.3% of the inter-annual variation in climate (Figure 1a). PC1 was dominated by inter-annual differences in temperature and precipitation, regardless of season, and the three components of temperature (mean, min and max) loaded similarly onto this component (Figure 1b). Over the last century, PC1 trends have fluctuated, with prolonged stretches of warm and dry years (the 1950s and early 2000s) and other periods of cool and wet years (early 1900s and 1970s–1980s), though the overall temporal trend for PC1 was negative. The decline per-year was nearly five times stronger since 1970 compared to the long-term average (Figure 1c), suggesting an accelerating trajectory of warmer and drier years. PC2 was strongly driven by cool-season climate, especially precipitation, such that greater values corresponded to wetter winters with low temperature maxima and high temperature minima (Figure 1b).

FIGURE 1 Principal component analysis (PCA) of inter-annual climate variability at SNWR, 1901–2017. (a) Proportion and cumulative proportion of variation in seasonal temperatures (minimum, mean maximum) and precipitation explained by the first three PCs. (b) Loadings of seasonal climate variables onto PC1–3. Because climate data were standardized to mean zero and unit variance, loadings can be interpreted as the correlation between the climate variable and the PC. (c–e) Time series of PC values, with regression lines showing long-term trends since 1901 (solid lines) or 1970 (dashed lines); open and filled points indicate the years 1970 and 2017, respectively, and correspond to the same shapes in Figure 3



Warm-season temperatures also loaded positively onto this axis to a lesser degree (Figure 1b). PC2 has increased since 1900 and the change per-year was nearly four times stronger since 1970 (Figure 1d), indicating an accelerating trend of wetter cool seasons with moderate winter temperatures. Lastly, PC3 was correlated with a combination of warm- and cool-season climate variables. The strongest variable loadings on this component were minimum and mean temperatures in the cool season and warm-season precipitation. Temporal trends for PC3 showed weak declines since 1900, corresponding to milder winters with higher minimum and mean temperatures and wetter warm seasons; this trend has been slightly stronger since 1970 (Figure 1e).

3.2 | Vital rate responses to climate

Demographic vital rates estimated from long-term data (survival, growth, reproductive status and fertility of flowering plants) were least responsive to PC1, the dominant axis of climate variability and change. All of the vital rates were strongly, positively size-dependent but there was heterogeneity in the magnitude and sign of responses to different dimensions of climate variability. Figure 2 shows vital rate data and fitted statistical models following variable selection procedures (Table B1). There was very little support for coefficients of quadratic climate effects (Table B1), indicating that responses to climate were monotonic over the range of variation we observed.

For PC1, there was a weak reduction in survival probability (especially for smaller plants; Figure 2a) and a moderate reduction in flowering probability (especially for larger plants; Figure 2g) at higher PC values, that is, in cooler and wetter years. Fertility of flowering plants was not responsive to PC1 variation (Figure 2j) and growth was not responsive to any of the climate PCs (Figure 2d–f). There were positive responses to PC2 in survival (Figure 2b), flowering probability (Figure 2h) and fertility of flowering plants (Figure 2k), indicating that these vital rates benefitted from years with wetter cool seasons. Responses to PC3 varied in sign, with survival increasing with decreasing PC values (years with mild winter temperature minima and wet summers) and reproductive rates increasing with increasing PC values (years with low winter minima and dry summers; Figure 2c, i and l).

3.3 | Climate-dependent population growth

The population growth rate λ was predicted to increase with decreasing values of PC1 (hotter, drier years), holding other PCs fixed at their long-term average (Figure 3a). Population growth was also predicted to increase with increasing values of PC2 (wetter cool seasons; Figure 3b). Population growth was more sensitive to PC2 than PC1, such that the predicted change in λ from 1970 to 2017 was slightly greater for PC2 even though PC1 exhibited much greater change than PC2 over this period. Finally, greater values

of PC3 (colder winters and drier summers) were predicted to cause declines in population growth, indicating that negative effects on cactus survival outweighed positive effects of PC3 on reproduction (Figure 2). PC3 has changed relatively little since 1970 but this was associated with a change in λ of about half the magnitude to the response to relatively large change in PC1. Overall, recent climate change in each of the principal components, in isolation, has been in the direction that favours increased population growth (Figures 1 and 3). However, mean estimates for population growth rates were consistently below replacement level for all climate PC values, and the posterior probability densities rarely met or exceeded $\lambda = 1$.

3.4 | Back-casting population growth

Figure 4a shows the back-casted time series of λ accounting for inter-annual variation in all three PC components. For the observation years (2004–2017), the three climate PCs explained 60% of the inter-annual variation in λ (points in Figure 4a). Thus, even with relatively strong climate–demography associations (Figure 2), there was substantial uncertainty in our back-casted estimates of λ . The shaded region in Figure 4a represents the combined uncertainty arising from heterogeneity in vital rates across years that could not be attributed to the climate PCs (process error) and imperfect knowledge of the underlying parameters (estimation error). In Appendix Figure C3, we show that process error contributed the majority of the total uncertainty.

Despite uncertainty in our back-cast, the results indicated that λ has likely remained below replacement levels for more than a century; there was no evidence that climate change drove this population into extinction debt. To the contrary, there was a positive temporal trend ($(\Delta\lambda/\Delta\text{Year}) > 0$), suggesting a trajectory of increasing population growth rates through time (Figure 4b). There was wide uncertainty in the rate of change but the posterior probability distribution indicated that it was three times more likely that λ has increased than decreased. Furthermore, the median rate of increase was 2.9 times greater since 1970 compared to the overall trend since 1900 (Figure 4b), corresponding to the acceleration of climate change (Figure 1). There was greater uncertainty in $(\Delta\lambda/\Delta\text{Year})$ since 1970 because this estimate was based on fewer years. Under the trajectory since 1970, population growth was expected to reach the viability threshold ($\lambda = 1$) in the year 2057 (Figure 4c); accelerating climate change would advance this transition to viable growth rates.

In Appendix D, we show that our inference that λ is likely increasing in response to climate change holds even with a more conservative approach that does not extrapolate vital rate responses beyond the climate extremes of the observation years. Furthermore, in Appendix A, we show that year-specific estimates of λ were correlated between models built with downscaled climate data versus on-site meteorological measurements, for years in which they overlapped (Figures A7 and A8). This suggests that

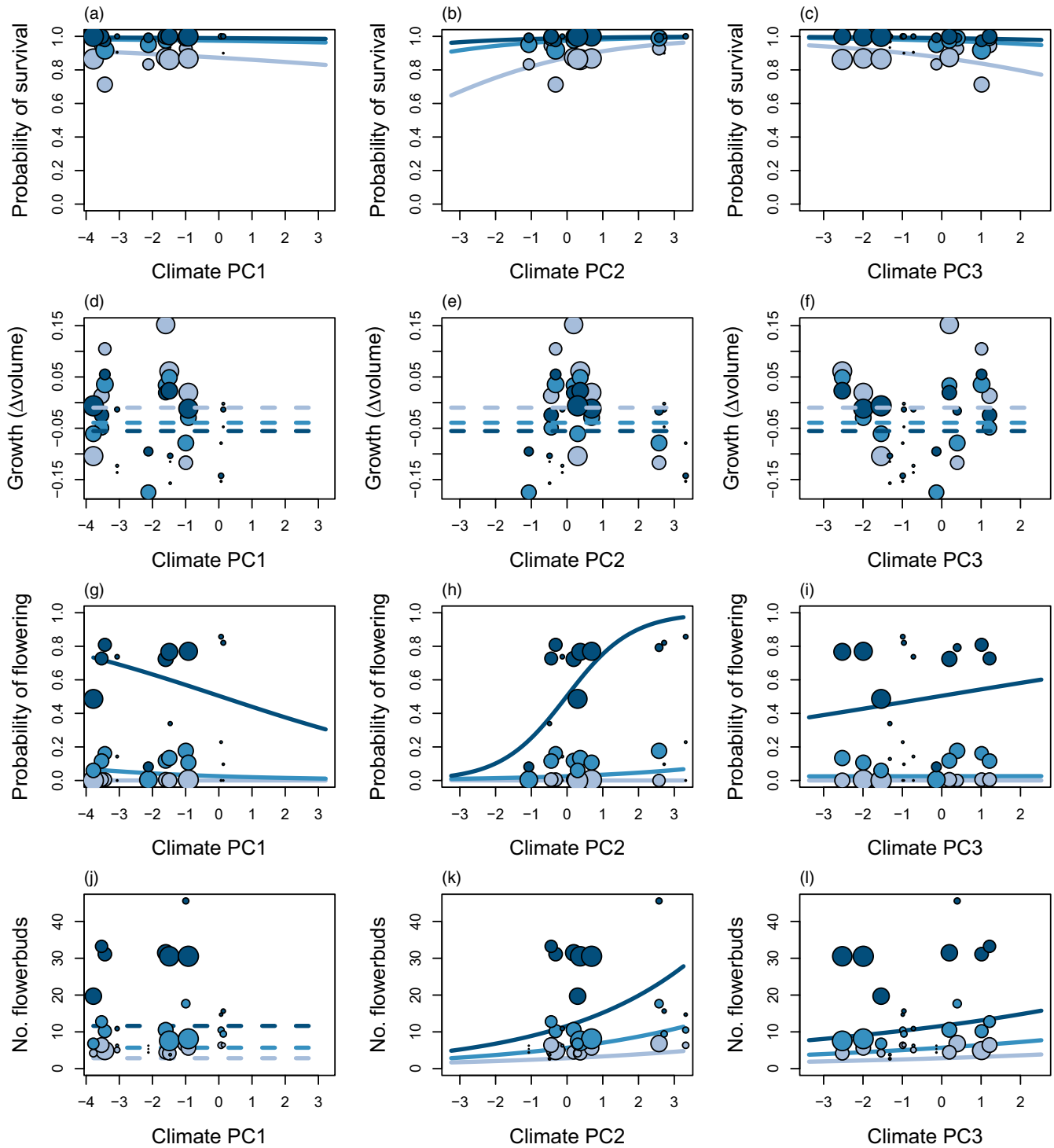


FIGURE 2 Climate- and size-dependent variation in survival (a–c), growth (d–f), flowering (g–i) and fertility of flowering plants (j–l) in relation to three principal components of seasonal climate variation (columns). For visualization only, the plant size distribution was discretized into three groups (small, medium and large, corresponding to increasingly dark shading). Points show means for each size group in each year, where different years have unique PC values and point size is proportional to sample size for each size group in each year. Lines show fitted statistical models using posterior mean parameter values, with shading corresponding to size groups. Dashed lines indicate that the climate predictor was not statistically supported. Ranges of x-axes show the climate extrapolation that was required for back-casting

our qualitative inference regarding the positive temporal trend in λ is robust to the loss of resolution associated with downscaled climate data.

The stochastic population growth rate (λ_s) showed a similar trend of $\lambda_s < 1$ and increasing population growth rates over the past 120 years (Figure C4). The stochastic growth rate reveals the effects

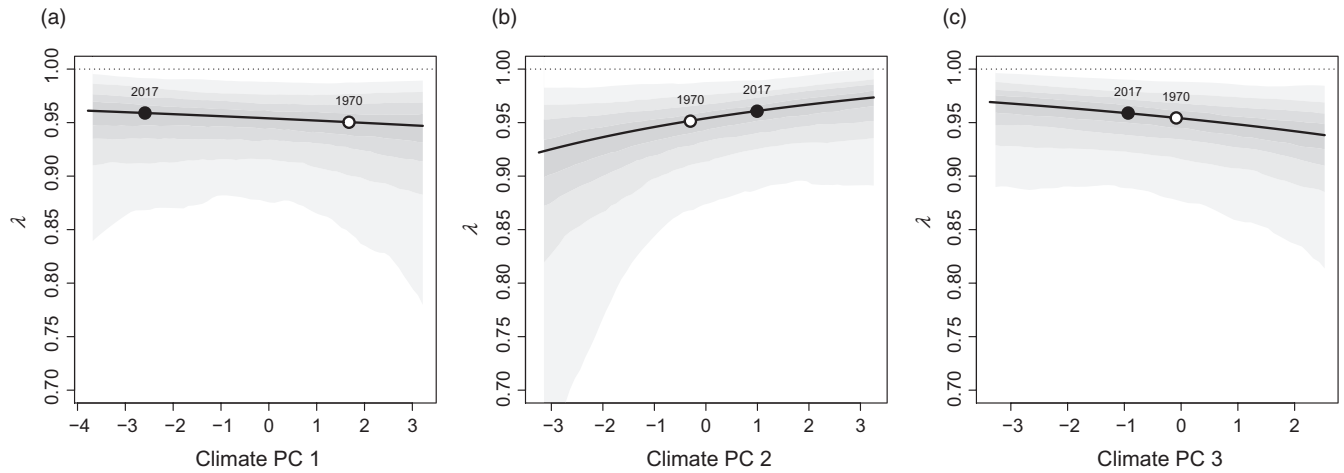


FIGURE 3 Predicted asymptotic population growth rate (λ) in response to three principal components of inter-annual climatic variation (a–c). For each panel, the indicated principal component is varying while the others are held at zero (the average value). Lines show the expected relationships based on posterior mean parameter values and shaded contours show the 25%, 50%, 75% and 95% credible intervals, representing uncertainty in demographic parameters. Points emphasize the change the PC value (on the x-axis) between 1970 and 2017, based on the regression lines shown in Figure 1, and the predicted corresponding change in λ (y-axis)

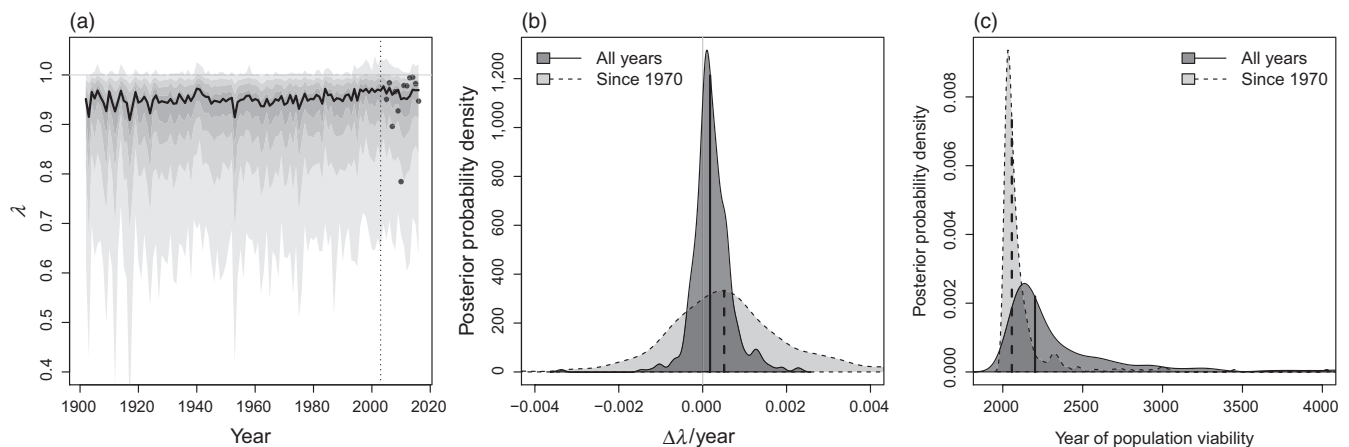


FIGURE 4 (a) Posterior probability distribution for the time series of asymptotic population growth rates (λ) predicted based on inter-annual variation in three climate PCs. Thick black line shows the mean prediction and shaded regions show the 25%, 50%, 75% and 95% credible regions accounting for both parameter uncertainty and process error (year-to-year variation in vital rates that was unrelated to climate). Dashed vertical line separates years that were back-casted versus years that were directly observed. The observation years (2004 and later) include estimates for year-specific population growth rates (points), captured statistically as year-specific random effects in the vital rates. (b) Posterior distributions for the rate of temporal change in population growth ($\Delta\lambda/\Delta\text{Year}$). Dark grey shows the rate of change across all years shown in A and light grey shows the rate of change since 1970. Vertical lines show median values. (c) Posterior distributions for the year of population viability ($\lambda = 1$) for the subset of posterior samples for which $(\Delta\lambda/\Delta\text{Year}) > 0$. Shading and lines as in b

of multi-year climate events, such as the runs of good years in the 1940s and 2000s.

3.5 | Life table response experiment

Life table response experiments (LTREs) provided a decomposition of how λ responded to long-term climate trends (1900–2017), allowing us to understand the relative importance of different dimensions of climate variability and vital rate responses to

them. LTRE results indicated that survival responses to climate were the overwhelming driver of temporal trends in λ (Figure 5). Individual growth made no contribution to these trends because it was unresponsive to climate (Figure 2D,E,F), whereas flowering and fertility were responsive to climate but their role was relatively small and imperceptible in Figure 5. Furthermore, survival responses to climate PC2 were the dominant driver of temporal trends, followed by PC3 and then PC1. Collectively, responses to PC2 and PC3 accounted for 90% of the overall climate effect in back-casted values of λ .

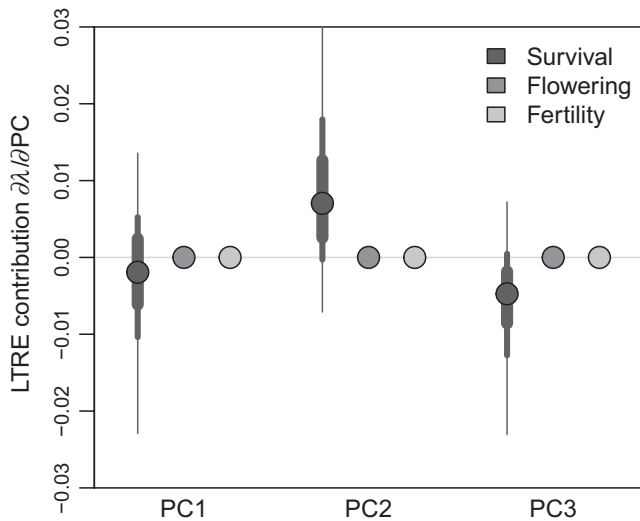


FIGURE 5 Life table response experiment (LTRE) decomposition of climate-driven inter-annual variability in population growth rates. Lines of decreasing thickness show the 50, 75 and 95 percentiles of the posterior distributions of the vital rate parameters, and points show the median. Shading corresponds to different vital rates (survival, flowering and fertility) Posterior distributions for flowering and fertility are imperceptible on this scale

4 | DISCUSSION

Understanding and predicting the effects of environmental change on plant demography and population dynamics are urgent challenges. The integration of long-term data with environmentally explicit demographic models provides a powerful vehicle for meeting these challenges and may aid in identifying processes that drive some populations into decline. By reconstructing 117 years of climate-dependent demography, we tested the hypothesis that the extinction debt of our study population was a consequence of recent climate change. Our results fail to support this hypothesis and suggest the opposite: *C. imbricata* is likely a climate change ‘winner’, on an accelerating trajectory towards replacement-level population growth within 37 years if current climate change trends persist, and sooner if they accelerate. We further show that the strongest feature of climate change in this system was not the main driver of population responses. Instead, temporal trends in population viability were dominated by more subtle climatic factors with relatively weak signals of recent change. Below, we interpret these results in greater detail and discuss their broader significance.

Until recently, few plant demographic studies explicitly considered climatic drivers of inter-annual variation (Crone et al., 2011; Ehrlén et al., 2016), though this is rapidly changing. We are aware of no previous studies that have compared the magnitudes of different aspects of climate change alongside the magnitudes of demographic responses to those changes. However, we suspect that our key finding—that the strongest dimension of climate change was not the strongest driver of demography—may be common, since

at the heart of this result lies the difference between annual climate trends (captured by PC1) versus seasonal trends (PCs 2 and 3). Annual rainfall totals in our region have been decreasing but more of the annual rainfall has been falling in the cool season, consistent with previous climatological studies that suggest a shift from warm- to cool-season precipitation (Cook, Ault, & Smerdon, 2015; Cook & Seager, 2013; Petrie, Collins, Gutzler, & Moore, 2014). Similarly, annual temperatures have been increasing in our study region but it was cool-season warming, specifically, that was most important for *C. imbricata* demography. Many plant and animal life histories operate on seasonal schedules and may therefore be more sensitive to seasonal redistribution of rainfall and temperature than to climate effects that manifest over an entire year. Our results are consistent with previous studies that demonstrate the importance of considering seasonal, not annual, drivers of plant demographic responses (Dahlgren, Bengtsson, & Ehrlén, 2016; Selwood, McGeoch, & Mac Nally, 2015; Williams et al., 2015). Some recent studies have taken a finer-grained approach, connecting plant responses to weather events on monthly, weekly or even daily time-scales (Shriver, 2016; Teller, Adler, Edwards, Hooker, & Ellner, 2016; Tenhumberg et al., 2018) or tractability, we did not explore lagged climate effects beyond one year, though methods for doing so are rapidly developing (Ogle et al., 2015; Teller et al., 2016; Tenhumberg et al., 2018). Finding the appropriate timing and resolution of climate covariates is an important area for future work in this system and more generally.

Rigorously accounting for various types of uncertainty is another an important area in the development of environmentally explicit models for forecasting or back-casting. Even with strong climate-demography relationships detected with our unusually long-term dataset, climate drivers accounted for less than two thirds of the inter-annual variation in λ during the study years. It was therefore important to place our predictions for historical growth rates in the context of the substantial uncertainty that arose from process error: all the additional, unspecified ways that years may differ. We have emphasized the positive trajectory of population viability as the most likely trend in λ , but this should be interpreted in light of the probability distributions that we provide (Figure 4)—that is, with nuance and appropriate caution.¹ As ecologists are increasingly called upon to forecast responses to change in climate drivers, it will be essential to do so in a probabilistic framework that accommodates process error, that is, the variability not explained by climate drivers. Defining the temporal or spatial auto-correlation structure of process error (which we did not attempt) may further improve forecasts or back-casts.

Different aspects of a species' life cycle may respond in diverse ways to environmental drivers (Doak & Morris, 2010; Villellas, Doak, García, & Morris, 2015), highlighting the additional importance of considering multiple vital rates for understanding responses to global change. Our work was able to pinpoint which responses

¹The probability that λ is increasing was approximately equal to the probability of a Clinton victory in the 2016 US presidential election: <https://projects.fivethirtyeight.com/2016-election-forecast/>

throughout the life cycle were most important for the overall population response to climate. Our results are consistent with previous findings that high-sensitivity vital rates (those that strongly influence λ , in this case survival and growth) are buffered against environmental variability while low-sensitivity vital rates (flowering and fertility) may exhibit wide fluctuations (Pfister, 1998). However, incomplete buffering of survival led to greater mortality in years with cold and dry cool-seasons—years that are becoming less frequent under climate change (Figure 1)—and these survival responses dominated the overall increase in population viability over the past 120 years (Figure 5). These results mirror a recent study of another long-lived perennial plant, the alpine sunflower *Helianthella quinquinervis*, where reproductive responses to climate drivers were strong but ultimately overwhelmed by weaker responses in survival that more strongly affected population growth (Iler et al., 2019). It is commonly observed that demographic transitions related to growth and survival are the most important determinants of population viability in species with long-lived perennial life histories (Franco & Silvertown, 2004). It may therefore be a general result that climate effects on growth and survival will be more consequential in long-lived perennials than effects on reproductive processes, even as the latter exhibit greater sensitivity to climate, since perennials have many reproductive opportunities over potentially long life spans (Dalglish, Koons, & Adler, 2010; Morris et al., 2008).

Our historical reconstruction of climate-dependent population growth indicated that the climate has likely never been better for *C. imbricata* than it is now. This result begs the question of how these plants have reached their current, relatively high abundance, given over a century of population growth rates that were inferred to fall well below replacement levels. Land use history—which is not incorporated into our back-casted estimates—may have played a role. The Sevilleta NWR was exposed to grazing for much of the 20th century until 1973. Previous work suggests that cacti, and *C. imbricata* in particular, can increase in abundance in response to grazing, due to livestock dispersing detached stem segment and thus promoting asexual regeneration (Allen, Allen, Kunst, & Sosebee, 1991). During our study, we observed recruitment to be almost exclusively from seed (sexual and asexual recruits are easily distinguishable), though it is possible that regeneration dynamics were different under historical grazing regimes. Grazing may have also promoted cactus populations through the release of competitive interactions with grasses (Yu et al., 2019). Thus, one hypothesis is that *C. imbricata* achieved current densities under the historical land use regime, and cannot maintain these densities in the absence of cattle grazing. For long-lived plants, it may take decades to centuries for full payment of extinction debt driven by land use changes (González-Varo, Albaladejo, Aizen, Arroyo, & Aparicio, 2015; Lehtilä et al., 2016). An alternative hypothesis is that, independent of grazing or other land use history, our study population may be located in sink habitat and maintained by dispersal from nearby populations that are more viable. Indeed, previous work showed that *C. imbricata* at lower (by c. 100 m) elevations had positive population growth rates (Miller et al., 2009)

and may therefore act as source populations. Regardless of which process or processes best account for the persistence of a population that is currently inviable, our results indicate that it will more likely than not be 'rescued' by ongoing climate change. One caveat to this conclusion is that, beyond the mean climate trends we have described, future climate (and especially monsoon precipitation) in our region is expected to be more variable (Cook et al., 2015; Rudgers et al., 2018) and this may dampen population growth independently of mean conditions (Boyce, Haridas, & Lee, 2006). However, our stochastic demographic analysis, which accounts for increasing climate variability during the 20th century, also showed a positive trajectory of λ_s (Figure C4).

Previous studies of cacti have emphasized their sensitivity to freezing as a constraint on physiological performance and geographic distribution (Flores & Yeaton, 2003; Kinraide, 1978; Nobel, 1984). In our study, we detected an important role for winter minimum temperature and observed high mortality following record low winter temperatures over a multi-day deep-freeze in 2011 (this is the low outlier in Figure 4a). As these freezing events become less frequent under climate change, we expect an increase in regional abundance and perhaps northern expansion of *C. imbricata*'s range, which currently extends to southern Colorado and is likely limited by winter minimum temperatures. This may be an issue of applied concern in the region since *C. imbricata* is considered undesirable due to its unpalatability to livestock (Allen et al., 1991). The role of cool-season precipitation that we detected was more surprising. A majority of annual precipitation in the Southwest United States comes from warm-season monsoon events (Adams & Comrie, 1997) and these events play a critical role in vegetation dynamics (Notaro & Gutzler, 2012; Petrie et al., 2014), especially for plants with C4 and CAM photosynthesis that are physiologically most active during the warm summer months. Previous cactus demographic studies have emphasized the role of summer monsoon precipitation (Bowers, 2005; Winkler, Conner, Huxman, & Swann, 2018). Our results suggest that, despite its summer-adapted CAM photosynthetic pathway, *C. imbricata* is able to capitalize on cool-season moisture, and this was an important component of the positive demographic effects of recent climate change. Similarly, Salguero-Gomez, Siewert, Casper, and Tielbörger (2012) identified *Cryptantha flava* as a species likely to benefit from climate change due in part to seasonal redistribution of rainfall that will lengthen its growing season.

Our work highlights several considerations that may be relevant for studies of demographic back-casting in other systems. First, we faced a trade-off between temporal depth and local resolution of climate data. While downscaled climate interpolation (from ClimateWNA) and on-site measurements (from SEV-LTER) were correlated, they were not perfectly so (Appendix A); this was especially true for temperature minima and maxima (Table A1), where downscaled data likely mis-estimate localized extremes. We prioritized the greater temporal coverage provided by downscaled data, which led an 18% reduction in how well climate explained inter-annual variation in λ , relative to on-site climate data (Appendix A). Consequently,

reliance on downscaled data inflated the contribution of process error to our back-casted estimates (Appendix D), and made λ appear less responsive to climate than it likely was. It is particularly noteworthy that the downscaled climate data poorly captured the deep-freeze of winter 2011 (Figure A1a). Poor demographic performance in this year was consequently attributed to a statistical random effect (Figure 4a), though this was almost certainly a true climate effect. As expected, the on-site data predicted a lower λ value in this year than the downscaled data (Figure A8). When available, climate data sources that break the trade-off between temporal depth and local resolution would provide the strongest foundation for accurate back-casting. When such resources are not available, quantifying the loss of resolution, as we have done (Appendix A), may be valuable for interpreting results.

Second, just like forecasting, demographic back-casting may require projection into climatic conditions that were represented poorly or not at all during the data collection period. This requires the assumption that the relationship between vital rates and climate covariates does not change or break down under conditions more extreme than observed. We found similar results whether or not we extrapolated demographic performance into unobserved conditions (Appendix D). This was a lucky break, reflecting the fact that the climate covariate requiring the most extrapolation (PC1) had the weakest effect on λ . In other cases, where important covariates must be extrapolated to no-analogue conditions, comparing results with and without extrapolation (Appendix D) may be valuable for setting liberal and conservative bounds on model projections. This approach may also aid in identifying situations where experimental climate manipulations could help bridge the gap between current and historic (or future) conditions.

Some additional limitations of our study warrant consideration in the interpretation of our results. First, our treatment of climate dependence was limited to four vital rate processes of established plants. Because we could not reliably assign a birth year to new recruits, we did not incorporate climate dependence in seedling recruitment. Previous studies of cactus demography suggest that seedling recruitment may be highly sensitive to climate, especially monsoon precipitation (e.g. Bowers, 2005; Winkler et al., 2018). We suspect this is the case for *C. imbricata*, since germination usually coincides with late-summer rains (T.E.X. Miller, unpubl. data). Because we did not model this process as climate-dependent, our results for climate effects on population growth are conservative. However, consistent with expectations for long-lived perennials, we know seedling recruitment to have very low eigenvalue sensitivities (Elder & Miller, 2016), which suggests that even large climate effects on this process may not strongly register in terms of population growth. On the other hand, pulsed recruitment events perturb the size distribution in ways that can importantly affect short-term (transient) dynamics (Williams, Ellis, Bricker, Brodie, & Parsons, 2011), and may therefore warrant further study in this and other pulsed-recruitment systems.

To conclude, this study illustrates how long-term patterns of population growth can be reconstructed (with potentially substantial

but quantifiable uncertainty) through climate–demography relationships observed on relatively short time-scales. This allowed us to evaluate the hypothesis that recent climate change has driven *C. imbricata* in our region into extinction debt, a hypothesis that our data do not support. Instead, this species is most likely benefitting from climate change, largely due to its positive responses, especially in survival, to recent and ongoing shifts in cool-season temperature and precipitation. Changes in cool-season climate were not the strongest features of climate change, but they were nonetheless the most important determinants of population responses. The more general lesson for global change biologists is that relatively subtle dimensions of climate change may trigger strong ecological responses.

ACKNOWLEDGEMENTS

This study was supported by the Sevilleta LTER (NSF LTER awards 1440478, 1655499 and 1748133) and by NSF Division of Environmental Biology awards 1543651 and 1754468. We thank the Sevilleta National Wildlife Refuge staff (especially J. Erz) for facilitating research access. We thank M. Evans and E. Schultz for helpful discussions on modelling climate–demography relationships and J. Williams for input on the manuscript. Finally, we thank the students and colleagues who have contributed to this long-term study, especially M. Donald, A. Compagnoni and B. Ochocki. Two reviewers provided valuable feedback on our work.

AUTHORS' CONTRIBUTIONS

T.E.X.M. initiated and maintained the long-term study; K.C. and T.E.X.M. collected and analysed the data and prepared a manuscript draft; T.E.X.M. finalized text and analyses. Both the co-authors approved this submission.

DATA AVAILABILITY STATEMENT

Our long-term data on tree cholla demography are publicly available (Miller, 2020b). Code for our statistical and demographic modelling is available at https://github.com/texmiller/cholla_climate_IPM (Miller, 2020a).

ORCID

Tom E. X. Miller  <https://orcid.org/0000-0003-3208-6067>

REFERENCES

- Ådahl, E., Lundberg, P., & Jonzen, N. (2006). From climate change to population change: The need to consider annual life cycles. *Global Change Biology*, 12, 1627–1633. <https://doi.org/10.1111/j.1365-2486.2006.01196.x>
- Adams, D. K., & Comrie, A. C. (1997). The North American monsoon. *Bulletin of the American Meteorological Society*, 78, 2197–2214. [https://doi.org/10.1175/1520-0477\(1997\)078<2197:TNAM>2.0.CO;2](https://doi.org/10.1175/1520-0477(1997)078<2197:TNAM>2.0.CO;2)
- Adler, P. B., Byrne, K. M., & Leiker, J. (2013). Can the past predict the future? Experimental tests of historically based population models. *Global Change Biology*, 19, 1793–1803. <https://doi.org/10.1111/gcb.12168>

- Allen, L., Allen, E., Kunst, C., & Sosebee, R. (1991). A diffusion model for dispersal of *Opuntia imbricata* (cholla) on rangeland. *The Journal of Ecology*, 79(4), 1123–1135.
- Bowers, J. E. (2005). Influence of climatic variability on local population dynamics of a Sonoran desert *Platyopuntia*. *Journal of Arid Environments*, 61, 193–210. <https://doi.org/10.1016/j.jaridenv.2004.09.003>
- Boyce, M., Haridas, C., Lee, C., & NCEAS Stochastic Demography Working Group. (2006). Demography in an increasingly variable world. *Trends in Ecology & Evolution*, 21, 141–148. <https://doi.org/10.1016/j.tree.2005.11.018>
- Buckley, L. B., & Kingsolver, J. G. (2012). The demographic impacts of shifts in climate means and extremes on alpine butterflies. *Functional Ecology*, 26, 969–977. <https://doi.org/10.1111/j.1365-2435.2012.01969.x>
- Caswell, H. (2001). *Matrix population models* (2nd ed.). Sunderland, MA: Sinauer Associates Inc.
- Compagnoni, A., Bibian, A. J., Ochocki, B. M., Rogers, H. S., Schultz, E. L., Sneck, M. E., ... Miller, T. E. X. (2016). The effect of demographic correlations on the stochastic population dynamics of perennial plants. *Ecological Monographs*, 86, 480–494. <https://doi.org/10.1002/ecm.1228>
- Cook, B. I., Ault, T. R., & Smerdon, J. E. (2015). Unprecedented 21st century drought risk in the American southwest and central plains. *Science Advances*, 1, e1400082. <https://doi.org/10.1126/sciadv.1400082>
- Cook, B., & Seager, R. (2013). The response of the North American monsoon to increased greenhouse gas forcing. *Journal of Geophysical Research: Atmospheres*, 118, 1690–1699. <https://doi.org/10.1002/jgrd.50111>
- Crone, E. E., Menges, E. S., Ellis, M. M., Bell, T., Bierzychudek, P., Ehrlén, J., ... Williams, J. L. (2011). How do plant ecologists use matrix population models? *Ecology Letters*, 14, 1–8. <https://doi.org/10.1111/j.1461-0248.2010.01540.x>
- Dahlgren, J. P., Bengtsson, K., & Ehrlén, J. (2016). The demography of climate-driven and density-regulated population dynamics in a perennial plant. *Ecology*. <https://doi.org/10.1890/15-0804.1>
- Dalgleish, H. J., Koons, D. N., & Adler, P. B. (2010). Can life-history traits predict the response of forb populations to changes in climate variability? *Journal of Ecology*, 98, 209–217. <https://doi.org/10.1111/j.1365-2745.2009.01585.x>
- Dalgleish, H. J., Koons, D. N., Hooten, M. B., Moffet, C. A., & Adler, P. B. (2011). Climate influences the demography of three dominant sagebrush steppe plants. *Ecology*, 92, 75–85. <https://doi.org/10.1890/10-0780.1>
- Daly, C., Halbleib, M., Smith, J. I., Gibson, W. P., Doggett, M. K., Taylor, G. H., ... Pasteris, P. P. (2008). Physiographically sensitive mapping of climatological temperature and precipitation across the conterminous United States. *International Journal of Climatology*, 28, 2031–2064. <https://doi.org/10.1002/joc.1688>
- Doak, D. F., & Morris, W. F. (2010). Demographic compensation and tipping points in climate-induced range shifts. *Nature*, 467, 959. <https://doi.org/10.1038/nature09439>
- Dullinger, S., Gatttringer, A., Thuiller, W., Moser, D., Zimmermann, N. E., Guisan, A., ... Hülber, K. (2012). Extinction debt of high-mountain plants under twenty-first-century climate change. *Nature Climate Change*, 2, 619. <https://doi.org/10.1038/nclimate1514>
- Dybala, K. E., Eadie, J. M., Gardali, T., Seavy, N. E., & Herzog, M. P. (2013). Projecting demographic responses to climate change: Adult and juvenile survival respond differently to direct and indirect effects of weather in a passerine population. *Global Change Biology*, 19, 2688–2697. <https://doi.org/10.1111/gcb.12228>
- Ehrlén, J., & Morris, W. F. (2015). Predicting changes in the distribution and abundance of species under environmental change. *Ecology Letters*, 18, 303–314. <https://doi.org/10.1111/ele.12410>
- Ehrlén, J., Morris, W. F., von Euler, T., & Dahlgren, J. P. (2016). Advancing environmentally explicit structured population models of plants. *Journal of Ecology*, 104, 292–305. <https://doi.org/10.1111/1365-2745.12523>
- Elder, B. D., & Miller, T. E. X. (2016). Quantifying demographic uncertainty: Bayesian methods for integral projection models. *Ecological Monographs*, 86, 125–144.
- Flores, J. L., & Yeaton, R. (2003). The replacement of arborescent cactus species along a climatic gradient in the southern Chihuahuan desert: Competitive hierarchies and response to freezing temperatures. *Journal of Arid Environments*, 55, 583–594. [https://doi.org/10.1016/S0140-1963\(02\)00288-4](https://doi.org/10.1016/S0140-1963(02)00288-4)
- Franco, M., & Silvertown, J. (2004). A comparative demography of plants based upon elasticities of vital rates. *Ecology*, 85, 531–538.
- Franklin, S. B., Gibson, D. J., Robertson, P. A., Pohlmann, J. T., & Fralish, J. S. (1995). Parallel analysis: A method for determining significant principal components. *Journal of Vegetation Science*, 6, 99–106. <https://doi.org/10.2307/3236261>
- Frederiksen, M., Daunt, F., Harris, M. P., & Wanless, S. (2008). The demographic impact of extreme events: Stochastic weather drives survival and population dynamics in a long-lived seabird. *Journal of Animal Ecology*, 77, 1020–1029. <https://doi.org/10.1111/j.1365-2656.2008.01422.x>
- González-Varo, J. P., Albaladejo, R. G., Aizen, M. A., Arroyo, J., & Aparicio, A. (2015). Extinction debt of a common shrub in a fragmented landscape. *Journal of Applied Ecology*, 52, 580–589. <https://doi.org/10.1111/1365-2664.12424>
- Hastings, A., Abbott, K. C., Cuddington, K., Francis, T., Gellner, G., Lai, Y. C., ... Zeeman, M. L. (2018). Transient phenomena in ecology. *Science*, 361, eaat6412. <https://doi.org/10.1126/science.aat6412>
- Hijmans, R. J., Cameron, S. E., Parra, J. L., Jones, P. G., & Jarvis, A. (2005). Very high resolution interpolated climate surfaces for global land areas. *International Journal of Climatology*, 25, 1965–1978. <https://doi.org/10.1002/joc.1276>
- Hylland, K., & Ehrlén, J. (2013). The mechanisms causing extinction debts. *Trends in Ecology & Evolution*, 28, 341–346. <https://doi.org/10.1016/j.tree.2013.01.010>
- Iler, A. M., Compagnoni, A., Inouye, D. W., Williams, J. L., CaraDonna, P. J., Anderson, A., & Miller, T. E. X. (2019). Reproductive losses due to climate change-induced earlier flowering are not the primary threat to plant population viability in a perennial herb. *Journal of Ecology*, 107, 1931–1943. <https://doi.org/10.1111/1365-2745.13146>
- Jenouvrier, S., Caswell, H., Barbraud, C., Holland, M., Stroeve, J., & Weimerskirch, H. (2009). Demographic models and IPCC climate projections predict the decline of an emperor penguin population. *Proceedings of the National Academy of Sciences of the United States of America*, 106, 1844–1847. <https://doi.org/10.1073/pnas.0806638106>
- Jenouvrier, S., Holland, M., Stroeve, J., Serreze, M., Barbraud, C., Weimerskirch, H., & Caswell, H. (2014). Projected continent-wide declines of the emperor penguin under climate change. *Nature Climate Change*, 4, 715. <https://doi.org/10.1038/nclimate2280>
- Kinraide, T. B. (1978). The ecological distribution of cholla cactus (*Opuntia imbricata* (Haw.) DC.) in El Paso County, Colorado. *The Southwestern Naturalist*, 117–133. <https://doi.org/10.2307/3669987>
- Kuussaari, M., Bommarco, R., Heikkinen, R. K., Helm, A., Krauss, J., Lindborg, R., ... Steffan-Dewenter, I. (2009). Extinction debt: A challenge for biodiversity conservation. *Trends in Ecology & Evolution*, 24, 564–571. <https://doi.org/10.1016/j.tree.2009.04.011>
- Lehtilä, K., Dahlgren, J. P., Garcia, M. B., Leimu, R., Syrjänen, K., & Ehrlén, J. (2016). Forest succession and population viability of grassland plants: Long repayment of extinction debt in *Primula veris*. *Oecologia*, 181, 125–135. <https://doi.org/10.1007/s00442-016-3569-6>
- Lynch, H. J., Rhoads, M., Calabrese, J. M., Cantrell, S., Cosner, C., & Fagan, W. F. (2014). How climate extremes not means define a species'

- geographic range boundary via a demographic tipping point. *Ecological Monographs*, 84, 131–149. <https://doi.org/10.1890/12-2235.1>
- Maschinski, J., Baggs, J. E., Quintana-ascencio, P. F., & Menges, E. S. (2006). Using population viability analysis to predict the effects of climate change on the extinction risk of an endangered limestone endemic shrub, *Arizona cliffrose*. *Conservation Biology*, 20, 218–228. <https://doi.org/10.1111/j.1523-1739.2006.00272.x>
- McLean, N., Lawson, C. R., Leech, D. I., & van de Pol, M. (2016). Predicting when climate-driven phenotypic change affects population dynamics. *Ecology Letters*, 19, 595–608. <https://doi.org/10.1111/ele.12599>
- Miller, T. E. X. (2020a). Data from: Demographic back-casting reveals that subtle dimensions of climate change have strong effects on population viability. *Zenodo*, <https://doi.org/10.5281/zenodo.3924640>
- Miller, T. E. X. (2020b). *Long-term study of tree cholla demography in the Los Pinos mountains, Sevilleta National Wildlife Refuge*. <https://doi.org/10.6073/PASTA/DD06DF3F950AFE4A4642306182237D13>. Retrieved from <https://portal.edirepository.org/nis/mapbrowse?packa geid=knb-lter-sev.323.1>
- Miller, T. E. X., Louda, S. M., Rose, K. A., & Eckberg, J. O. (2009). Impacts of insect herbivory on cactus population dynamics: Experimental demography across an environmental gradient. *Ecological Monographs*, 79, 155–172. <https://doi.org/10.1890/07-1550.1>
- Morris, W. F., Pfister, C. A., Tuljapurkar, S., Haridas, C. V., Boggs, C. L., Boyce, M. S., ... Menges, E. S. (2008). Longevity can buffer plant and animal populations against changing climatic variability. *Ecology*, 89, 19–25. <https://doi.org/10.1890/07-0774.1>
- Morrison, S. F., & Hik, D. S. (2007). Demographic analysis of a declining pika *Ochotona collaris* population: Linking survival to broad-scale climate patterns via spring snowmelt patterns. *Journal of Animal Ecology*, 76, 899–907. <https://doi.org/10.1111/j.1365-2656.2007.01276.x>
- Nobel, P. S. (1984). Extreme temperatures and thermal tolerances for seedlings of desert succulents. *Oecologia*, 62, 310–317. <https://doi.org/10.1007/BF00384262>
- Notaro, M., & Gutzler, D. (2012). Simulated impact of vegetation on climate across the North American monsoon region in CCSM3. 5. *Climate Dynamics*, 38, 795–814. <https://doi.org/10.1007/s0038 2-010-0990-0>
- Ogle, K., Barber, J. J., Barron-Gafford, G. A., Bentley, L. P., Young, J. M., Huxman, T. E., ... Tissue, D. T. (2015). Quantifying ecological memory in plant and ecosystem processes. *Ecology Letters*, 18, 221–235. <https://doi.org/10.1111/ele.12399>
- Ohm, J. R., & Miller, T. E. X. (2014). Balancing anti-herbivore benefits and anti-pollinator costs of defensive mutualists. *Ecology*, 95, 2924–2935. <https://doi.org/10.1890/13-2309.1>
- Peters, D. P., Havstad, K. M., Archer, S. R., & Sala, O. E. (2015). Beyond desertification: New paradigms for dryland landscapes. *Frontiers in Ecology and the Environment*, 13, 4–12. <https://doi.org/10.1890/140276>
- Petrie, M., Collins, S., Gutzler, D., & Moore, D. (2014). Regional trends and local variability in monsoon precipitation in the northern Chihuahuan desert, USA. *Journal of Arid Environments*, 103, 63–70. <https://doi.org/10.1016/j.jaridenv.2014.01.005>
- Pfister, C. A. (1998). Patterns of variance in stage-structured populations: Evolutionary predictions and ecological implications. *Proceedings of the National Academy of Sciences of the United States of America*, 95, 213–218. <https://doi.org/10.1073/pnas.95.1.213>
- Plummer, M. (2003). Jags: A program for analysis of Bayesian graphical models using Gibbs sampling. In *Proceedings of the 3rd International Workshop on Distributed Statistical Computing*, Vienna, Austria, Vol. 124, No. 125, 10 pp.
- Rudgers, J. A., Chung, Y. A., Maurer, G. E., Moore, D. I., Muldavin, E. H., Litvak, M. E., & Collins, S. L. (2018). Climate sensitivity functions and net primary production: A framework for incorporating climate mean and variability. *Ecology*, 99, 576–582. <https://doi.org/10.1002/ ecy.2136>
- Salguero-Gomez, R., Siewert, W., Casper, B. B., & Tielbörger, K. (2012). A demographic approach to study effects of climate change in desert plants. *Philosophical Transactions of the Royal Society B: Biological Sciences*, 367, 3100–3114. <https://doi.org/10.1098/rstb.2012. 0074>
- Selwood, K. E., McGeoch, M. A., & Mac Nally, R. (2015). The effects of climate change and land-use change on demographic rates and population viability. *Biological Reviews*, 90, 837–853. <https://doi.org/10.1111/ brv.12136>
- Shriver, R. K. (2016). Quantifying how short-term environmental variation leads to long-term demographic responses to climate change. *Journal of Ecology*, 104, 65–78. <https://doi.org/10.1111/1365-2745.12490>
- Sletvold, N., Dahlgren, J. P., Øien, D. I., Moen, A., & Ehrlén, J. (2013). Climate warming alters effects of management on population viability of threatened species: Results from a 30-year experimental study on a rare orchid. *Global Change Biology*, 19, 2729–2738. <https://doi.org/10.1111/gcb.12167>
- Smith, M., Caswell, H., & Mettler-Cherry, P. (2005). Stochastic flood and precipitation regimes and the population dynamics of a threatened floodplain plant. *Ecological Applications*, 15, 1036–1052. <https://doi.org/10.1890/04-0434>
- Su, Y. S., & Yajima, M. (2012). *R2jags: A package for running jags from R*. R package version 0.03-08. Retrieved from <http://CRAN.R-proje ct.org/package=R2jags>
- Teller, B. J., Adler, P. B., Edwards, C. B., Hooker, G., & Ellner, S. P. (2016). Linking demography with drivers: Climate and competition. *Methods in Ecology and Evolution*, 7, 171–183. <https://doi.org/10.1111/2041-210X.12486>
- Tenhumberg, B., Crone, E. E., Ramula, S., & Tyre, A. J. (2018). Time-lagged effects of weather on plant demography: Drought and *Astragalus scaphoides*. *Ecology*, 99, 915–925.
- Urban, M. C. (2015). Accelerating extinction risk from climate change. *Science*, 348, 571–573. <https://doi.org/10.1126/science.aaa4984>
- Van de Pol, M., Vindenes, Y., Sæther, B. E., Engen, S., Ens, B. J., Oosterbeek, K., & Tinbergen, J. M. (2010). Effects of climate change and variability on population dynamics in a long-lived shorebird. *Ecology*, 91, 1192–1204. <https://doi.org/10.1890/09-0410.1>
- Vellend, M., Verheyen, K., Jacquemyn, H., Kolb, A., Van Calster, H., Peterken, G., & Hermy, M. (2006). Extinction debt of forest plants persists for more than a century following habitat fragmentation. *Ecology*, 87, 542–548. <https://doi.org/10.1890/05-1182>
- Villellas, J., Doak, D. F., García, M. B., & Morris, W. F. (2015). Demographic compensation among populations: What is it, how does it arise and what are its implications? *Ecology Letters*, 18, 1139–1152. <https://doi.org/10.1111/ele.12505>
- Wang, T., Hamann, A., Spittlehouse, D., & Carroll, C. (2016). Locally downscaled and spatially customizable climate data for historical and future periods for North America. *PLoS ONE*, 11, e0156720. <https://doi.org/10.1371/journal.pone.0156720>
- Williams, J. L., Ellis, M. M., Bricker, M. C., Brodie, J. F., & Parsons, E. W. (2011). Distance to stable stage distribution in plant populations and implications for near-term population projections. *Journal of Ecology*, 99, 1171–1178. <https://doi.org/10.1111/j.1365-2745.2011.01845.x>
- Williams, J. L., Jacquemyn, H., Ochocki, B. M., Brys, R., & Miller, T. E. X. (2015). Life history evolution under climate change and its influence on the population dynamics of a long-lived plant. *Journal of Ecology*, 103, 798–808.
- Williams, J. L., Miller, T. E. X., & Ellner, S. P. (2012). Avoiding unintentional eviction from integral projection models. *Ecology*, 93, 2008–2014. <https://doi.org/10.1890/11-2147.1>
- Winkler, D. E., Conner, J. L., Huxman, T. E., & Swann, D. E. (2018). The interaction of drought and habitat explain space time patterns of establishment in saguaro (*Carnegiea gigantea*). *Ecology*, 99, 621–631.
- Yu, K., D'Odorico, P., Collins, S. L., Carr, D., Porporato, A., Anderegg, W. R., ... Hartzell, S. (2019). The competitive advantage of a constitutive

CAM species over a C4 grass species under drought and CO₂ enrichment. *Ecosphere*, 10, e02721.

SUPPORTING INFORMATION

Additional supporting information may be found online in the Supporting Information section.

How to cite this article: Czachura K, Miller TEX. Demographic back-casting reveals that subtle dimensions of climate change have strong effects on population viability. *J Ecol.* 2020;00: 1-14. <https://doi.org/10.1111/1365-2745.13471>